Dynamic and static quenching of 2-aminopurine fluorescence by the natural DNA nucleotides in solution

PAPER • **OPEN ACCESS**

Dynamic and static quenching of 2-aminopurine fluorescence by the natural DNA nucleotides in solution

Methods and Applications in Fluorescence

PAPER

Dynamic and static quenching of 2-aminopurine fluorescence by the natural DNA nucleotides in solution

Kyle A Paterson[1], Jochen Arlt[2] and Anita C Jones[1]

[1] EaStCHEM School of Chemistry, University of Edinburgh, Joseph Black Building, David Brewster Road, Edinburgh EH9 3FJ, United Kingdom

[2] School of Physics and Astronomy, University of Edinburgh, James Clerk Maxwell Building, Peter Guthrie Tait Road, Edinburgh EH9 3FD, United Kingdom

E-mail: a.c.jones@ed.ac.uk

OPEN ACCESS

RECEIVED
4 September 2019

REVISED
24 November 2019

ACCEPTED FOR PUBLICATION
30 January 2020

PUBLISHED
19 February 2020

Keywords: 2-aminopurine, DNA base, nucleoside monophosphate, base stacking, fluorescence quenching, charge transfer, Stern-Volmer equation

Supplementary material for this article is available online

Abstract

2-aminopurine (2AP) is a responsive fluorescent base analogue that is used widely as a probe of the local molecular environment in DNA. The ability of 2AP to report changes in local conformation and base-stacking interactions arises from the efficient quenching of its fluorescence by the natural DNA bases. However, the mechanism of this inter-base quenching remains imperfectly understood. Two previous studies of the collisional quenching of 2AP by the natural bases, in different buffer solutions, showed that dynamic quenching efficiency depends on the identity of the natural base, but disagreed on the relative quenching efficiencies of the bases. We report a comprehensive investigation of inter-base quenching of 2AP by the natural nucleoside monophosphates (NMPs), replicating the buffer conditions used in the previous studies. Using time-resolved fluorescence measurements to distinguish between dynamic and static quenching, we find that the dynamic quenching rate constants of the different bases show a consistent trend across both buffers, and this is in line with a charge-transfer mechanism. Time-resolved measurements also provide insight into static quenching, revealing formation of 2AP-NMP ground-state complexes in which 2AP displays a very short fluorescence lifetime, comparable to that seen in oligonucleotides. In these complexes, the dependence of the rate of quenching on the partner base also supports a charge-transfer mechanism.

1. Introduction

DNA is increasingly recognised as playing new and unforeseen roles in biochemical processes, not just as a store of genetic information, but also undergoing repair and epigenetic modification, suggesting a more complex web of interactions rather than the traditional linear transcription-translation model. Understanding these processes in more detail is often achieved using fluorescent probes inserted at specific sites in DNA strands, exploiting the high sensitivity and noninvasive nature of fluorescence spectroscopy. 2-aminopurine (2AP) (scheme 1) is one such probe that is used extensively in studies of DNA structure and DNA-enzyme interactions [1]. 2AP is a fluorescent analogue of adenine that forms Watson-Crick base pairs with thymine; its structure differs from that of the natural base only in the position of the exocyclic amino group and yet its fluorescence quantum yield is greater by 3 orders of magnitude. When 2AP is inserted into an oligonucleotide its fluorescence is highly quenched by interaction with the natural bases, making it an extraordinarily sensitive fluorescent probe of nucleic acid structure.

Several early studies of the photophysics of 2AP in DNA showed that the fluorescence is quenched by stacking with the natural bases and the quenching efficiency is sensitive to the identity of the neighbouring bases and the local duplex conformation [2–5]. Barton and co-workers established that 2AP fluorescence is quenched efficiently by photoinduced electron transfer from guanine and took advantage of this effect in their studies of the mechanism of charge transfer in DNA (see, for example, Kelley [6] and O'Neill and

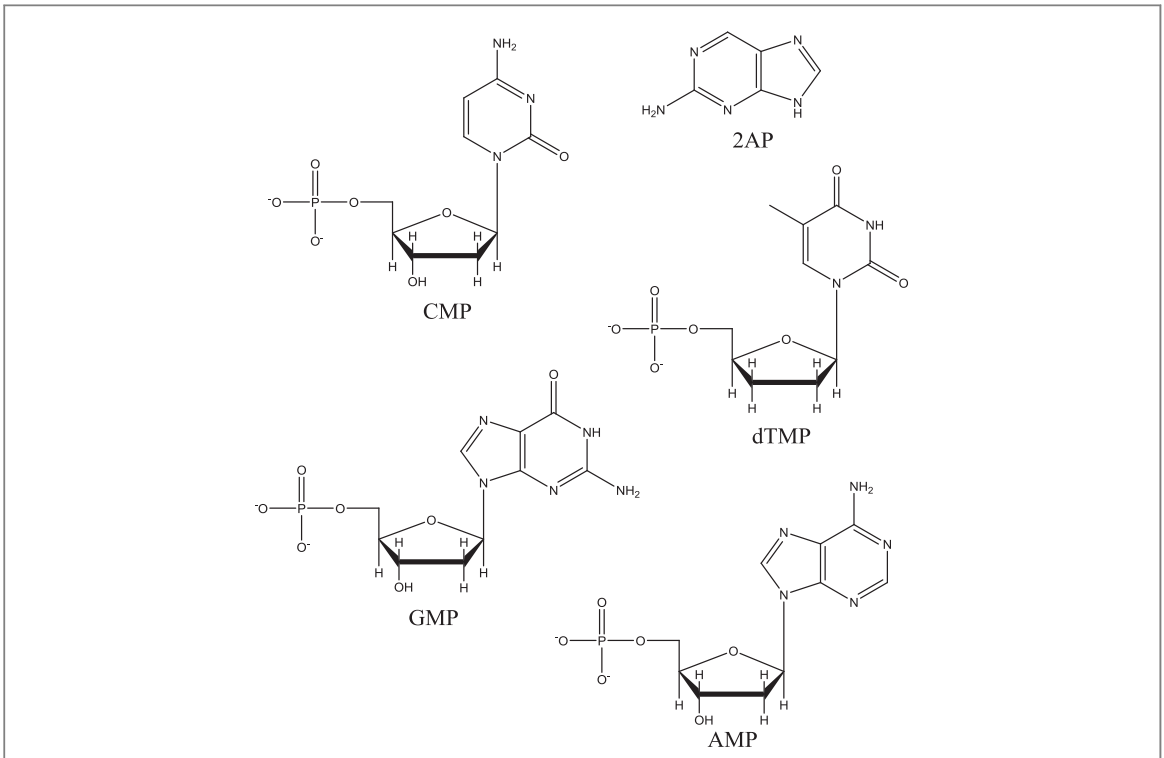

Scheme 1. Structures of 2-aminopurine (2AP) and the DNA nucleotides, cytidine-5′-monophosphate (CMP), deoxythymidine-5′-monophosphate (dTMP), guanosine-5′-monophosphate (GMP) and adenosine-5′-monophosphate (AMP).

Barton [7–13]). Other fluorophores, including fluorescent dyes and Au nanoclusters, have been found to be quenched by photoinduced electron transfer with guanine, and this effect has been exploited in biosensing applications [14–17].

Further information on the quenching interaction between the natural bases and 2AP came from steady-state and time-resolved fluorescence studies of 2AP-containing deoxydinucleotides [18, 19]. These showed that the fluorescence quantum yield of 2AP depends on the identity of the natural base with which it is stacked, increasing in the order G $\ll$ T $<$ A, C. An ultrafast spectroscopic study of 2AP-containing dinucleotides and non-covalent complexes, with G, A and 7-deaza guanine (Z), found that relative decay rates, Z $>$ G $>$ A, were consistent with non-radiative decay via a charge-transfer state [20]. More recent computational studies of π-stacked dimers of 2AP with the natural nucleobases (in the gas phase) [21, 22] confirmed the importance of charge-transfer character in the mechanism of fluorescence quenching and identified quenching pathways involving charge-transfer exciplex states or conical intersections with charge-transfer character.

In an early time-resolved fluorescence study of the effects of local environment on 2AP fluorescence, Rachofsky *et al* [23] investigated collisional (Stern-Volmer) quenching by the natural nucleosides in aqueous buffer solution. Dynamic quenching rate constants determined from fluorescence lifetime measurements were similar in magnitude for all four nucleosides (ranging from 1.7×10^9 to 2.2×10^9 $M^{-1}s^{-1}$), with the lowest value observed for guanosine and the highest for adenosine. This is the inverse of the order of quenching efficiencies found in dinucleotides (*vide supra*). In a more recent study, Narayanan *et al* [24] used steady-state fluorescence measurements, together with cyclic voltammetry, to show that photoinduced electron transfer is the most likely mechanism for quenching of 2AP fluorescence by the natural nucleosides. The reported dynamic quenching rate constants are similar in magnitude to those of Rachofsky *et al* [23], but vary more widely between the different nucleosides (ranging from 1.4×10^9 to 2.5×10^9 $M^{-1}s^{-1}$) and show the highest value for G, decreasing in the order G $>$ T $>$ A, C. This trend in quenching efficiency is in agreement with that reported for dinucleotides and is consistent with a charge-transfer mechanism.

The discrepancy between the results of these two Stern-Volmer quenching studies is disturbing and casts doubt on the validity of this attractively simple approach as a means to investigate the susceptibility of fluorescent base analogues to inter-base quenching. The main difference between the studies is in the buffer that was used: 20 mM Tris-HCl (pH 7.5) in the earlier study and 0.1 M phosphate (pH 7.0) in the later one. This suggested that the solvent environment may affect the quenching process.

In an effort to resolve these conflicting reports, we have carried out a comprehensive investigation of quenching of 2AP by the natural nucleoside monophosphates (scheme 1), in both buffer systems. We have used time-resolved fluorescence, in addition to steady-state measurements, to determine definitive

dynamic quenching constants. We find that the dynamic quenching rate constants show a consistent trend across both buffers, and this is in line with a charge-transfer mechanism. We uncover shortcomings in both previous studies. Time-resolved measurements also provide insight into static quenching, revealing formation of ground-state complexes in which 2AP displays a very short fluorescence lifetime; this is comparable to sub-100 ps decay times that are observed in 2AP-containg oligonucleotides, and can be attributed to highly stacked conformations [1, 25].

2. Experimental

2.1. Materials

Adenosine-5′-monophosphate disodium salt (AMP), 2-aminopurine (2AP) and cytidine-5′-monophosphate disodium salt (CMP) were purchased from Sigma. Deoxythymidine-5′-monophosphate disodium salt (dTMP) was purchased from Abcam. Guanosine-5′-monophosphate disodium salt (GMP) was purchased from Acros Organics. These were all used as received.

HPLC grade water (Fisher) was used as the solvent throughout. Measurements were made in phosphate buffer (0.1 M, pH 7) and Tris-HCl buffer (20 mM Tris-HCl, 60 mM NaCl, 0.1 mM Na_2EDTA).

Samples of 2AP at a fixed concentration (~3 μM) and varying concentrations of nucleotides were prepared in either phosphate or Tris-HCl buffer.

2.2. Fluorescence measurements

Steady-state fluorescence measurements were performed on a Horiba Fluoromax-P photon-counting spectrofluorimeter and the resulting spectra were analysed using Origin graphing software. An excitation wavelength of 325 nm was used and emission intensity was corrected for variation in the excitation lamp intensity. The detector response was constant over the emission wavelength range used. Emission intensities were determined by integration over a 180-nm bandwidth encompassing the emission maximum, and were averaged over five measurements.

Fluorescence lifetimes were measured using time-correlated single photon counting on an Edinburgh Instruments spectrometer equipped with TCC900 photon counting electronics. The excitation source was the third harmonic of the pulse-picked output of a mode-locked Ti-Sapphire laser (Coherent Mira pumped by Coherent Verdi), consisting of pulses of ~150 fs duration at a repetition rate of 4.75 MHz and a wavelength of 310 nm. Fluorescence emission was detected orthogonal to the excitation beam through a polarizer set at the magic angle with respect to the vertically polarized excitation. A band-pass of 10 nm was used in the emission monochromator and photons were detected by a cooled microchannel plate detector (Hamamatsu R3809 series). The instrument response of the system was ~80 ps full-width at half-maximum. Fluorescence decay curves were recorded on a time scale of 50 ns, resolved into 4096 channels, to a total of 10,000 counts in the peak channel. Decay curves were analyzed by iterative re-convolution, assuming a multi-exponential function, equation (1), using Edinburgh Instruments software FAST.

$$I(t) = \sum_{i=1}^{n} A_i \exp\left(\frac{-t}{\tau_i}\right) \quad (1)$$

where I is the fluorescence intensity as a function of time, t, (normalised to the intensity at $t = 0$); τ_i is the fluorescence lifetime of the ith decay component and A_i is the fractional amplitude (A-factor) of that component.

2.3. Data analysis

The effect of a quencher, Q, on the fluorescence quantum yield of a fluorophore, M, can be expressed by the classical Stern-Volmer equation (2) [26].

$$\frac{\varnothing_0}{\varnothing} = 1 + K_{SV}[Q] \quad (2)$$

where $\varnothing_0$ and $\varnothing$ are the fluorescence quantum yields of M in the absence and presence of Q, respectively, [Q] is the molar concentration of Q, and K_{SV} is the Stern-Volmer constant.

If quenching is purely dynamic, i.e. occurs by collision of Q with excited M, K_{SV} is equal to the dynamic quenching constant, K_D, as defined in equation (3).

$$K_D = k_q \tau_0 \quad (3)$$

where k_q is the bimolecular rate constant for collisional quenching and τ_0 is the fluorescence lifetime of M in the absence of the quencher.

If quenching is purely static, i.e. occurs by interaction of M and Q in the ground state to form a complex, MQ, that has a fluorescence quantum yield less than that of free M, an average quantum yield is measured, as expressed by equation (4).

$$\langle\varnothing\rangle = \alpha\varnothing_0 + (1-\alpha)\varnothing_{MQ} \quad (4)$$

where $\langle\varnothing\rangle$ is the average quantum yield in the presence of quencher, $\varnothing_{MQ}$ is the quantum yield of MQ, and α is the fractional population of free M, as defined by equation (5).

$$\alpha = \frac{[M]}{[M] + [MQ]} = \frac{1}{1 + K_S[Q]} \quad (5)$$

where K_S, is the equilibrium constant for formation of MQ (equation (6)), and is known as the static quenching constant.

$$K_S = \frac{[MQ]}{[M][Q]} \quad (6)$$

If $\varnothing_{MQ} \ll \varnothing_0$, equation (4) reduces to equation (7), which is identical in form to the classical Stern-Volmer expression (equation (2)), with K_{SV} equal to the static quenching constant, K_S. This corresponds to the commonly expressed assumption that complexes MQ

are 'non-fluorescent' [26].

$$\frac{\varnothing_0}{\langle\varnothing\rangle} = 1 + K_S[Q] \quad (7)$$

If both static and dynamic quenching occur, their combined effects on the quantum yield are expressed by equation (8).

$$\langle\varnothing\rangle = \frac{\alpha\varnothing_0}{1 + K_D[Q]} + (1 - \alpha)\varnothing_{MQ} \quad (8)$$

If $\varnothing_{MQ} \ll \varnothing_0$, this becomes the modified Stern-Volmer equation (9).

$$\frac{\varnothing_0}{\langle\varnothing\rangle} = (1 + K_S[Q])(1 + K_D[Q]) \quad (9)$$

In steady-state fluorescence-quenching measurements, it is assumed that the ratio of the fluorescence intensity (I_0) of M in the absence of Q to that (I) in the presence of Q is equal to the corresponding quantum yield ratio. This assumption is valid provided that the intensity of excitation light absorbed by M is constant throughout the measurements.

Time-resolved fluorescence measurements permit the effects of dynamic and static quenching to be separated. Dynamic quenching is manifested by a decrease in the fluorescence lifetime of M with increasing concentration of Q, according to equation (10).

$$\frac{\tau_0}{\tau_M} = 1 + k_q\tau_0[Q] \quad (10)$$

where τ_0 and τ_M are the fluorescence lifetimes of M in the absence and presence of Q, respectively.

In the presence of static quenching, if the fluorescence lifetime of MQ is too short to be measurable (i.e. MQ is effectively non-fluorescent), then a mono-exponential decay will be observed with lifetime, τ_M. However, if the lifetime of MQ, τ_{MQ}, is measurable, an additional component will be seen in the fluorescence decay, as given by equation (11).

$$I(t) = \alpha\exp\left(\frac{-t}{\tau_M}\right) + (1 - \alpha)\exp\left(\frac{-t}{\tau_{MQ}}\right) \quad (11)$$

where I is the fluorescence intensity as a function of time, t, (normalised to the intensity at $t = 0$); both α (defined in equation (4)) and τ_M (equation (10)) depend on [Q], but τ_{MQ} is independent of [Q].

The modified Stern-Volmer equation may then be expressed in terms of the number-average lifetime, $\langle\tau\rangle$.

$$\frac{\tau_0}{\langle\tau\rangle} = (1 + K_S[Q])(1 + k_q\tau_0[Q]) \quad (12)$$

where $\langle\tau\rangle = \alpha\tau_M + (1 - \alpha)\tau_{MQ}$.

3. Results and discussion

3.1. Measurements in Tris-HCl buffer

These measurements were made under the same buffer conditions as those used by Rachofsky *et al* [23], but we chose to use the natural bases in the form of the NMPs, rather than the nucleosides, because of their increased solubility. Furthermore, we used an excitation wavelength of 325 nm for our steady-state measurements, to minimise the inner filter effect that might occur due to absorption by the NMPs at high concentrations. Rachofsky *et al* [23] used an excitation wavelength of 309 nm, assuming negligible absorbance by the natural bases at this wavelength. However, although the molar absorption coefficients of the natural bases at this wavelength are very small, there is sufficient absorbance at concentrations of 10's of mM over a path-length of 0.5 cm to significantly attenuate the excitation intensity. This effect is greatest for GMP and TMP (see figures S1 and S2 of supplementary information, available online at stacks.iop.org/MAF/8/025002/mmedia), resulting in a decrease in intensity with increasing NMP concentration equivalent to K_{SV} values of ~14 M^{-1} and ~7 M^{-1}, respectively, and deviation from linearity at concentrations above 0.03 M.

The dependence of the fluorescence intensity of 2AP on the concentration of each of the NMPs is shown in figure 1, in the form of a classic Stern-Volmer plot. The data could be fitted adequately by equation (2) yielding the values given in table 1 for the Stern-Volmer constant, K_{SV}. However, there may be small deviations from linearity, suggesting the occurrence of static quenching. Rachofsky *et al* [23] reported only dynamic quenching constants obtained from time-resolved fluorescence measurements. They indicated that they were unable to obtain static quenching constants because of the low solubility of the ribosides, but commented that upward curvature in Stern-Volmer plots of steady-state data was observed.

To obtain definitive dynamic quenching constants, we carried out time-resolved fluorescence measurements. An excitation wavelength of 310 nm (near the maximum of the 2AP absorption spectrum) was used, since the inner filter effect does not affect the fluorescence lifetime, only the fluorescence intensity. The decay parameters of 2AP measured as a function of GMP concentration are given in table 2.

For concentrations of GMP up to 1 mM, single exponential decays were observed, with the lifetime decreasing with increasing quencher concentration, as expected for dynamic quenching (equation (10)). However, above this concentration, an additional two, shorter, decay components (τ_2 and τ_3) appeared, which can be attributed to the onset of static quenching. The 3-component decays for GMP concentrations from 5 to 50 mM could be fitted globally with τ_2 and τ_3 as common (i.e. concentration-independent) lifetimes; the value of τ_1 decreases steadily with increasing GMP concentration. The fractional populations (A factors) of components τ_2 and τ_3 increase with increasing GMP concentration. This is consistent with a model in which τ_1 is due to free 2AP undergoing dynamic quenching by GMP, while τ_2 and τ_3 are due to two photophysically distinct 2AP-GMP complexes,

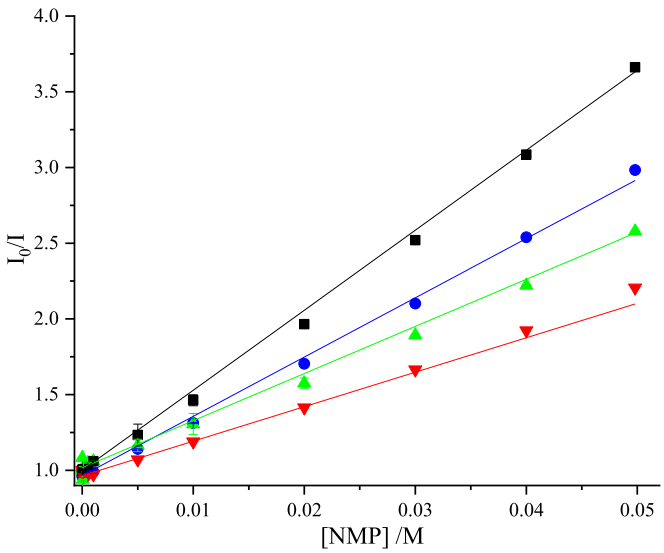

Figure 1. Stern-Volmer plots of fluorescence intensity data for quenching of 2AP fluorescence by the nucleoside monophosphates in Tris-HCl buffer. GMP (blue), dTMP (green), AMP (black), CMP (red). Experimental data are shown as points and fitted function (equation (2)) as solid line. In all cases, R^2 values were greater than 0.99.

Table 1. Stern-volmer constants, K_{SV}, determined from the steady-state fluorescence data shown in figures 1 and 3, in Tris-HCl and phosphate buffers.

	K_{SV} ($\pm\sigma$)/M^{-1}		
Nucleoside	Tris-HCl	Phosphate	Phosphate (Lit.)[a]
GMP	52.1 (0.5)	28.8 (0.3)	31.8
AMP	38.4 (0.7)	26.2 (0.3)	26.4
CMP	23.1 (0.6)	15.0 (0.2)	16.5
dTMP	30.8 (0.5)	19.2 (0.3)	23.4

[a] Values of K_{SV} in phosphate buffer derived from the results reported by Narayanan *et al* [24] are given, for comparison.

in which 2AP is statically quenched by GMP. The nature of the complexes (as reflected by their lifetimes) is independent of GMP concentration, but their populations increase as GMP concentration increases. In the τ_3 complex, 2AP is highly quenched by interaction with GMP to give a lifetime of only 60 ps. This is comparable to the very short lifetimes observed for 2AP stacked with G in DNA duplexes [1] and for the 2AP-G dinucleotide [19, 27], implying that there is intimate stacking of 2AP and G in the τ_3 complex. The much longer lifetime of the τ_2 complex suggests a structure in which there is much weaker interaction between 2AP and G, but still significant quenching. The fractional population of the τ_3 complex is much greater than that of the τ_2 complex, indicating that a well-stacked structure is favoured. This is in line with computational prediction of highly stacked structures for non-covalent complexes of 2AP and the natural bases [21, 22, 28].

Similar decay behaviour was observed for 2AP in the presence of the other NMPs, as shown in tables S1–S3 in the supplementary information. In all cases, two statically-quenched complex populations are observed at concentrations above 1 mM, a minor population with a lifetime (τ_2) of ~3 ns, and the major component with a much shorter lifetime (τ_3). The value of τ_3 depends on the identity of the natural base, and decreases in the order A > C > G ~ T, indicating a decrease in quenching efficiency in that order. In all cases, at a NMP concentration of 50 mM, the τ_3 complex accounts for ~30% of the emitting population, while τ_2 constitutes less than 10%. Although the statically quenched complexes show measurable fluorescence, their average quantum yield is no more than 3% that of unquenched 2AP.

The value of K_D, and hence k_q, (equation (3)) for each NMP was determined from a plot of $\frac{\tau_0}{\tau_M}$ versus [NMP] (equation (10)), where τ_M is the lifetime component τ_1. The linear fits are shown in figure 2 and the quenching constants are given in table 3.

We find that the rate constant for collisional quenching, k_q, is greater for GMP and dTMP than for AMP and CMP. Our k_q values for GMP and AMP differ significantly from those of Rachofsky *et al* [23]; we find that GMP has the greatest value of k_q, whereas they report that guanosine has the lowest k_q value and adenosine the highest. Rachofsky *et al* [23] do not present the fluorescence decay data that they used to obtain k_q values; however, it is evident that they observed multi-exponential decays at higher nucleoside concentrations, and we note that they incorrectly employed the intensity-average lifetime for Stern-Volmer analysis.

The considerable difference between the K_D values obtained from lifetime data (table 3) and the *Ksv* values obtained from the classic Stern-Volmer plots (table 1, figure 1) confirms the occurrence of static quenching. We used three alternative methods to determine the static quenching constant for each of

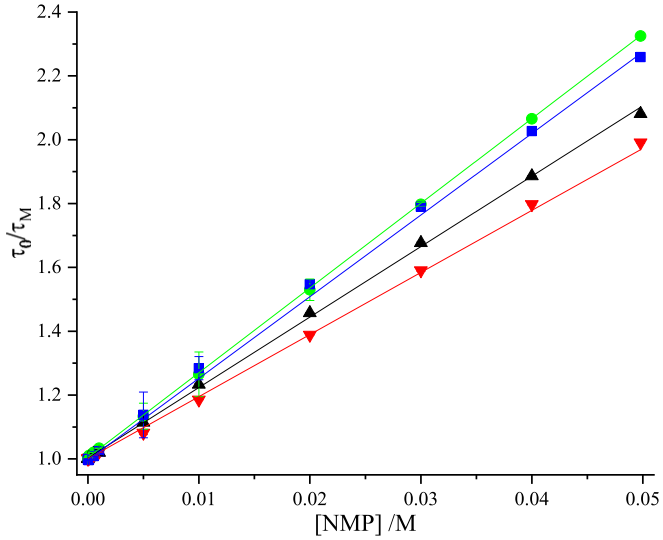

Figure 2. Stern-Volmer plots of fluorescence lifetime data for dynamic quenching of 2AP fluorescence by the nucleoside monophosphates in Tris-HCl buffer. GMP (blue), dTMP (green), AMP (black), CMP (red). Experimental data are shown as points and fitted function (equation (10)) as solid line. In all cases, R^2 values were greater than 0.99

Table 2. Fluorescence decay parameters for 2AP in Tris-HCl buffer as a function of concentration of GMP. 3-component decays for concentrations 5–50 mM were fitted globally with τ_2 and τ_3 as common lifetimes.

[GMP]/mM	τ_1/ns	τ_2/ns	τ_3/ns	A_1	A_2	A_3	τ/ns
0	11.38	—	—	1.0	—	—	11.38
0.5	11.28	—	—	1.0	—	—	11.28
1.0	11.11	—	—	1.0	—	—	11.11
5.0	10.00	2.75	0.06	0.86	0.02	0.12	8.64
10	8.86	2.75	0.06	0.84	0.02	0.14	7.46
20	7.35	2.75	0.06	0.79	0.03	0.18	5.93
30	6.36	2.75	0.06	0.74	0.04	0.22	4.80
40	5.61	2.75	0.06	0.67	0.04	0.28	3.90
50	5.04	2.75	0.06	0.60	0.05	0.35	3.19

Table 3. Dynamic quenching constants obtained from fluorescence lifetime data for 2AP in the presence of the nucleoside monophosphates in Tris-HCl buffer.

.Nucleoside	K_D ($\pm\sigma$) /M^{-1}	$k_q/10^9$ M^{-1} s^{-1}	k_q (Lit.)[a]/109 M^{-1} s^{-1}
GMP	25.7 (0.3)	2.25 (0.05)	1.70 (0.13)
AMP	22.0 (0.2)	1.85 (0.04)	2.21 (0.10)
CMP	19.8 (0.2)	1.70 (0.04)	1.90 (0.03)
dTMP	26.5 (0.1)	2.22 (0.05)	2.14 (0.04)

[a] Literature values reported by Rachofsky *et al* [23] for the nucleosides are shown for comparison.

the NMPs: (i) fluorescence intensity data were fitted with the modified Stern-Volmer equation (equation (9)), with the value of K_D fixed; (ii) average lifetime data (tables 2 and S1–S3 of supplementary information) were fitted with the modified Stern-Volmer equation (equation (12)) with the value of K_D fixed; (iii) from linear plots of $1/\alpha$ versus [NMP] (equation (5)), where α, the fractional population of free 2AP, is obtained from decay data as the value of A_1 (table 2 and S1–S3 of supplementary information). Examples of (ii) and (iii) are shown for AMP in figures 3 and 4. The data and fits for the other NMPs are given in the supplementary information (figures S3 and S4). The values of K_s obtained are given in table 4. The values of K_S obtained from the two decay-data-based methods ($\tau_0/\langle\tau\rangle$ and $1/\alpha$) are in good agreement and are similar for all the NMPs, indicating a similar propensity for stacking with 2AP in all cases.

However, for CMP and dTMP, there is a significant discrepancy between these values and those

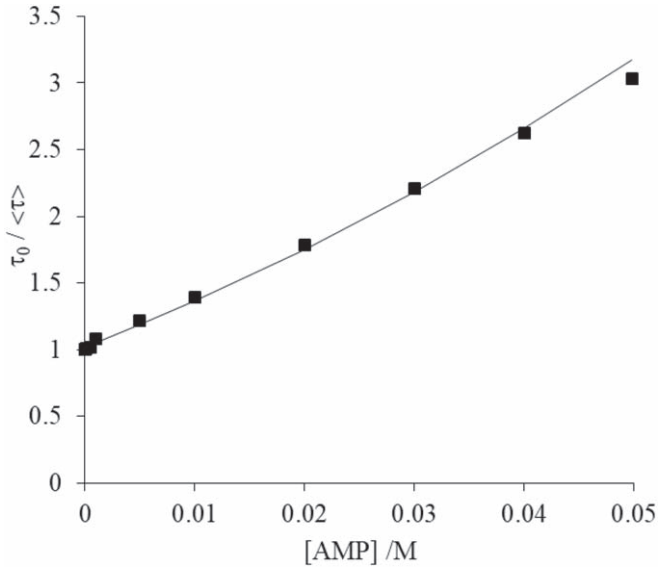

Figure 3. Average fluorescence lifetime data for quenching of 2AP by AMP in Tris-HCl buffer, fitted by the modified Stern-Volmer equation (equation (11)) with the value of K_D fixed. Experimental data are shown as points and fitted function as solid line. The R^2 value of the fit was 0.997. (Error bars are smaller than the data points).

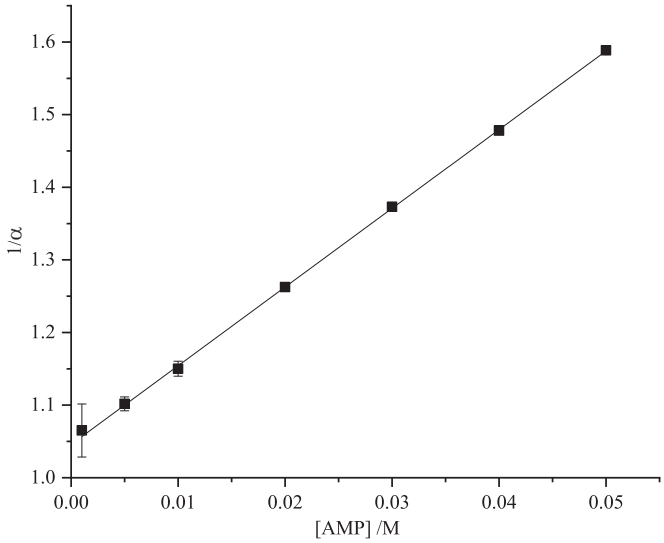

Figure 4. Plot of the inverse of the fractional population (α) of free 2AP as a function of AMP concentration, in Tris-HCl buffer. Experimental data are shown as points and the fitted function (see equation (5)) as solid line. The R^2 value of the fit was better than 0.99.

Table 4. Static quenching constants for 2AP in the presence of the nucleoside monophosphates in Tris-HCl buffer, obtained from intensity data, average lifetime data and fractional population data.

	$K_S (\pm\sigma)$ /M^{-1}		
Nucleoside	I_0/I	$\tau_0/\langle\tau\rangle$	$1/\alpha$
GMP	7.7 (0.2)	11.1 (0.4)	10.7 (1.0)
AMP	9.0 (0.2)	9.2 (0.3)	10.8 (0.1)
CMP	2.4 (0.2)	9.7 (0.2)	10.0 (0.7)
dTMP	3.7 (0.3)	10.0 (0.6)	8.9 (1.1)

obtained from intensity data. This suggests that I_0/I is not a reliable measure of relative quantum yield in these cases; the quantum yield of the complexes relative to free 2AP is overestimated. This would be accounted for by a greater molar absorption coefficient of 2AP in complex with these NMPs than that of free 2AP, at the excitation wavelength of 325 nm. Since we are exciting on the red edge of the 2AP absorption spectrum, a small complexation-induced spectral shift could result in a signifcant increase in absorption coefficient compared with free 2AP. It has been observed

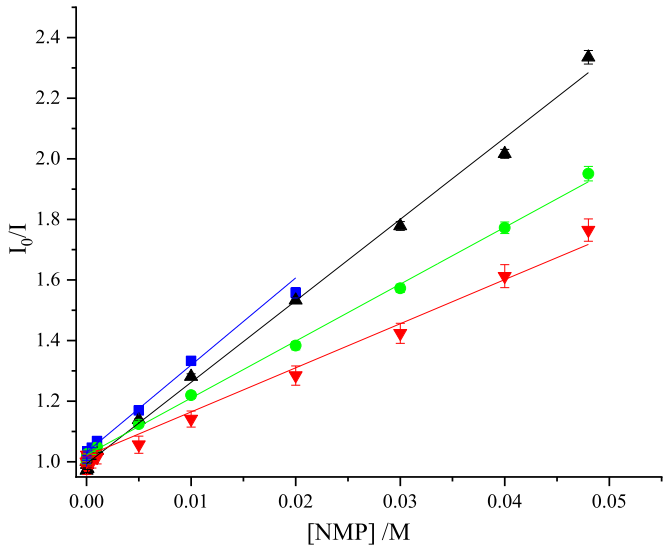

Figure 5. Stern-Volmer plots of fluorescence intensity data for quenching of 2AP fluorescence by the nucleoside monophosphates in 0.1 M phosphate buffer. GMP (blue), AMP (black), dTMP (green), CMP (red). Experimental data are shown as points and fitted function (equation (2)) as solid line. In all cases, R^2 values were $\geqslant$0.99. For GMP, data are limited to concentrations $\leqslant$0.02 M, as explained in the text.

previously that interbase stacking interactions lead to a red-shift of a few nm in the absoprtion or excitation spectrum of 2AP when it is inserted into oligonucleotides [29–31].

3.2. Measurements in phosphate buffer

To replicate the conditions used by Narayanan *et al* [24], the quenching of the fluorescence of the 2AP base by each of the natural nucleoside monophosphates was investigated in 0.1 M phosphate buffer.

The dependence of the fluorescence intensity of 2AP on the concentration of each of the NMPs is shown in the Stern-Volmer plots in figure 5, and could be fitted adequately by equation (2), yielding the values given in table 1 for the Stern-Volmer constant, K_{SV}. For GMP in this buffer, we saw evidence of G-quartet formation [32] (increase in viscosity of the solution and scattering of excitation light) at concentrations above 20 mM. Consequently, the analysis of quenching was restricted to lower concentrations, and this prevented the analysis of static quenching by GMP in this buffer. The formation of G-quartets, a form of self-aggregation unique to guanosine, is enhanced in this buffer system by the high concentration of potassium ions [32].

Narayanan *et al* [24] chose to fit their intensity data to the modified Stern-Volmer equation (equation (9)), with both K_D and K_S as variable parameters. They do not comment on the deviation from linearity of their data, and, since they present the data plotted on a logarithmic concentration scale, this cannot be discerned. However, we find that the functions fitted by Narayanan *et al* [24] can be very well approximated by linear Stern-Volmer functions (equation (2)) ($R^2 > 0.998$) over the range of concentrations measured (as shown in figure S5 of the supplementary information). This suggests that their data could be fitted adequately by the linear equation; indeed the values of K_S that they report are small ($<5\ M^{-1}$), with relatively high errors. The K_{SV} values that we estimate from their results, on that basis, are given in table 1. These values are in good agreement with those of the present work, and follow the same trend.

To further investigate the quenching process, the fluorescence decay of 2AP was measured as a function of NMP concentration. We found that the fluorescence lifetime of 2AP in this buffer, in the absence of NMP, is much shorter than expected, only 5.7 ns, half that in Tris-HCl buffer (table 2). This suggested that the buffer itself ($H_2PO_4^-/HPO_4^{2-}$) was acting as a quencher. This was confirmed by measurement of the lifetime as a function of buffer concentration (figure S6 of supplementary information), which demonstrated dynamic quenching, with $k_q = 1.00 \times 10^9\ M^{-1}\ s^{-1}$. To our knowledge the quenching of 2AP fluorescence by phosphate buffer has not been reported previously, although phosphate anions have been observed to quench the fluorescence of tryptophan and tyrosine [33–35]. Narayanan *et al* [24] were unaware of the quenching effect of the buffer and erroneously used a literature value of 11.4 ns for τ_0 in calculating k_q from K_D.

For AMP, CMP and dTMP, the effect of their concentration on the fluorescence decay parameters of 2AP was similar to that observed in Tris-HCl buffer, as shown in tables S4–S6 of supplementary information. Monoexponential decays at sub-mM NMP concentrations switch to 3-exponential decays at concentrations above 1 mM, with the onset of static quenching. The values of τ_2 and τ_3 are shorter than in Tris-HCl buffer, suggesting that the interaction between 2AP and the NMP in the statically quenched complexes is

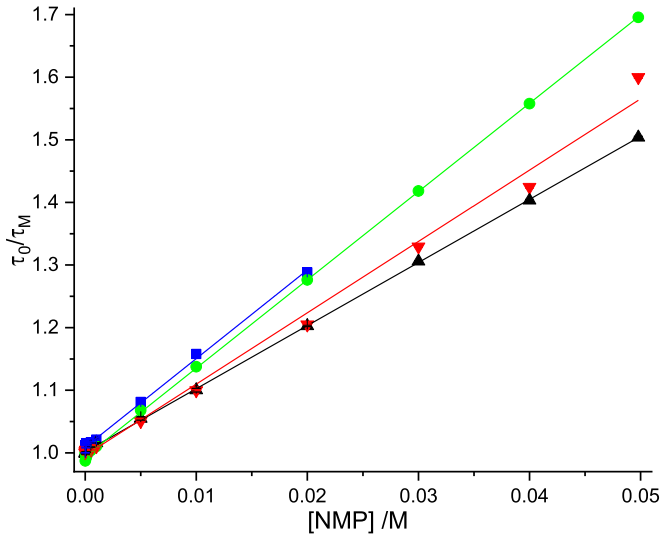

Figure 6. Stern-Volmer plots of fluorescence lifetime data for dynamic quenching of 2AP fluorescence by the nucleoside monophosphates in 0.1 M phosphate buffer. dTMP (green), GMP (blue), AMP (black), CMP (red). Experimental data are shown as points and the fitted function (equation (10)) as solid line. In all cases, R^2 values were greater than 0.99. For GMP, data are limited to concentrations $\leqslant$0.02 M, as explained in the text.

Table 5. Dynamic quenching constants obtained from fluorescence lifetime data for 2AP in the presence of the nucleoside monophosphates in 0.1 M phosphate buffer.

Nucleoside	$K_D\,(\pm\sigma)/M^{-1}$	$k_q/10^9\,M^{-1}\,s^{-1}$	k_q (Lit.)[a]$/10^9\,M^{-1}\,s^{-1}$
GMP	14.1 (0.3)	2.50 (0.05)	2.52 (0.72)
AMP	11.4 (0.2)	1.99 (0.03)	1.55 (0.42)
CMP	11.6 (0.2)	2.00 (0.02)	1.43 (0.41)
dTMP	14.2 (0.2)	2.50 (0.02)	1.71 (0.44)

[a] Literature values reported by Narayanan *et al* [16].

Table 6. Static quenching constants for 2AP in the presence of the nucleoside monophosphates in 0.1 M phosphate buffer, obtained from intensity data, average lifetime data and fractional population data.

	$K_S\,(\pm\sigma)\,/M^{-1}$			
Nucleoside	I_0/I	$\tau_0/\langle\tau\rangle$	$1/\alpha$	I_0/I (Lit)[a]
AMP	9.9 (0.4)	6.5 (0.2)	7.5 (0.3)	5.0 (1.0)
CMP	2.4 (0.2)	5.0 (0.9)	5.7 (0.5)	0.2 (1.2)
dTMP	3.6 (0.2)	5.9 (0.2)	6.0 (0.9)	2.2 (0.4)

[a] Literature values reported by Narayanan *et al* [24].

influenced by the composition of the buffer. Nevertheless, the trend in τ_3, A > C > G, T, is the same as seen in Tris-HCl.

For GMP, the decay parameters (table S7 of supplementary information) are anomalous due to G-quartet formation; this is manifested mainly as very high amplitudes of the shortest decay component at concentrations above 20 mM. (This may be due to some type of enhanced quenching process, but could be an artefact due to intense light scattering by the guanosine aggregates.) Therefore, the use of these decay data was restricted to the determination of the dynamic quenching constant at concentrations $\leqslant$20 mM.

The values of K_D and k_q determined from the lifetime data are given in table 5. The Stern-Volmer plots are shown in figure 6. As a consequence of the much shorter τ_0, the K_D vaues are approximately one half those measured in Tris-HCl (table 3), but the k_q values and their trend are very similar in both buffers. The values of k_q reported by Narajanan *et al* [24] are in surprisingly good agreement, given that they were calculated on the assumption of a τ_0 of 11.4 ns. However, this is merely a fortuitous consequence of their substantial overestimation of the K_D values from fits of intensity data to the modified Stern-Volmer equation.

Static quenching constants for AMP, CMP and dTMP were determined as described above, yielding the values shown in table 6. Related plots are shown in figures S7 and S8 of supplementary information. The values of K_S are comparable to those measured in Tris-HCl, although somewhat lower. Complexation appears to be less favourable in the phosphate buffer. A similar discrepancy between decay-derived and intensity-derived values is evident for CMP and

dTMP. The values reported by Narayanan *et al* [24] are significantly less than our values and show much greater variability between the nucleosides. This, together with the overstimation of K_D values (*vide supra*), is symptomatic of the correlation of variables inherent in unconstrained fitting of data with the modified Stern-Volmer equation.

4. Conclusions

Contrary to previous studies, we find that the dynamic quenching efficiencies of the NMPs follow the same trend in Tris-HCl and 0.1 M phosphate buffers. Rate constants for dynamic quenching of 2AP by GMP and dTMP are greater than those for quenching by AMP and CMP. This is consistent with a charge-transfer quenching mechanism. The nature of the buffer does, however, significantly affect the fluorescence lifetime of 2AP in the absence of the NMPs. In 0.1 M phosphate buffer the lifetime of 'unquenched' 2AP is one half that in Tris-HCl, as a result of dynamic quenching by phosphate anions, with a k_q of 1.0×10^9 M^{-1} s^{-1}. Surprisingly, this quenching process has not been reported previously and was not taken into account in the data analysis of Narayanan *et al* [24].

Time-resolved fluorescence measurements revealed the formation of highly quenched ground-state complexes between 2AP and the NMPs, with lifetimes comparable to those seen for 2AP in oligonucleotides. These solution-phase complexes evidently have a closely stacked structure, conducive to rapid quenching. The dependence of the rate of quenching on the NMP stacking partner mimics that seen in 2AP-containing dinucleotides and supports a charge-transfer mechanism. Static quenching constants indicate that all of the natural nucleotides have a similar propensity to stack with 2AP.

This work illustrates that time-resolved fluorescence measurements are not only important in the definitive analysis of dynamic quenching, but can also provide valuable insight into static quenching. In traditional Stern-Volmer analysis, statically quenched, ground-state complexes are treated as being 'non-fluorescent'. However, with ever-improving time-resolution in fluorescence lifetime measurements, species once deemed to be non-fluorescent can now readily be observed. Even with the relatively modest time-resolution of time-correlated single-photon counting, 2AP-NMP complexes with quantum yields a factor of a thousand less than unquenched 2AP have been detected and quantified, providing an alternative means of determining static quenching constants.

Finally, we conclude that, with rigorous execution, collisional quenching measurements can give useful insight into the mechanism of inter-base quenching and should be a valuable tool in the preliminary assessment of the responsiveness of new fluorescent base analogues to inter-base interactions.

Acknowledgments

This work was supported by the EPSRC and The University of Edinburgh, by the provision of a PhD studentship for KAP. Data associated with this paper are avaialable at https://doi.org/10.7488/ds/2717.

Conflicts of Interest

The authors have declared that no conflicting interests exist.

ORCID iDs

Jochen Arlt https://orcid.org/0000-0002-4152-5896
Anita C Jones https://orcid.org/0000-0002-7476-2214

References

[1] Jones A C and Neely R K 2015 2-Aminopurine as a fluorescent probe of DNA conformation and the DNA-enzyme interface *Q. Rev. Biophys.* **48** 244–79
[2] Guest C R, Hochstrasser R A, Sowers L C and Millar D P 1991 Dynamics of mismatched base pairs in DNA *Biochemistry* **30** 3271–9
[3] Nordlund T M, Andersson S, Nilsson L, Rigler R, Graeslund A and McLaughlin L W 1989 Structure and dynamics of a fluorescent DNA oligomer containing the EcoRI recognition sequence: fluorescence, molecular dynamics, and NMR studies *Biochemistry* **28** 9095–103
[4] Rachofsky E L, Seibert E, Stivers J T, Osman R and Ross J B A 2001 Conformation and dynamics of abasic sites in DNA investigated by time-resolved fluorescence of 2-aminopurine† *Biochemistry* **40** 957–67
[5] Xu D, Evans K O and Nordlund T M 1994 Melting and premelting transitions of an oligomer measured by DNA base fluorescence and absorption *Biochemistry* **33** 9592–9
[6] Kelley S O 1999 Electron transfer between bases in double helical DNA *Science* **283** 375–81
[7] O'Neil M A and Barton J K 2002 2-Aminopurine: a probe of structural dynamics and charge transfer in DNA and DNA: RNA hybrids *JACS* **124** 13053–66
[8] O'Neill M A and Barton J K 2002 Effects of strand and directional asymmetry on base-base coupling and charge transfer in double-helical DNA *Proc. Natl. Acad. Sci. U S A* **99** 16543–50
[9] O'Neill M A and Barton J K 2004 DNA-mediated charge transport requires conformational motion of the DNA bases: elimination of charge transport in rigid glasses at 77 K *J. Am. Chem. Soc.* **126** 13234–5
[10] O'Neill M A and Barton J K 2004 DNA charge transport: conformationally gated hopping through stacked domains *J. Am. Chem. Soc.* **126** 11471–83
[11] O'Neill M A, Becker H C, Wan C, Barton J K and Zewail A H 2003 Ultrafast dynamics in DNA-mediated electron transfer: base gating and the role of temperature *Angew. Chem. Int. Ed. Engl.* **42** 5896–900
[12] O'Neill M A, Dohno C and Barton J K 2004 Direct chemical evidence for charge transfer between photoexcited 2-aminopurine and guanine in duplex DNA *J. Am. Chem. Soc.* **126** 1316–7
[13] Wan C, Fiebig T, Schiemann O, Barton J K and Zewail A H 2000 Femtosecond direct observation of charge transfer between bases in DNA *Proc. Natl Acad. Sci.* **97** 14052–5

[14] Torimura M et al 2001 Fluorescence-quenching phenomenon by photoinduced electron transfer between a fluorescent dye and a nucleotide base Anal. Sci. 17 155–60
[15] Wang H-B, Bai H-Y, Dong G-L and Liu Y-M 2019 DNA-templated Au nanoclusters coupled with proximity-dependent hybridization and guanine-rich DNA induced quenching: a sensitive fluorescent biosensing platform for DNA detection Nanoscale Advances 1 1482–8
[16] Piestert O et al 2003 A single-molecule sensitive DNA hairpin system based on intramolecular electron transfer Nano Lett. 3 979–82
[17] Zhang L, Zhu J, Guo S, Li T, Li J and Wang E 2013 Photoinduced electron transfer of DNA/Ag nanoclusters modulated by G-Quadruplex/Hemin complex for the construction of versatile biosensors JACS 135 2403–6
[18] Larsen O F A et al 2004 Ultrafast transient-absorption and steady-state fluorescence measurements on 2-aminopurine substituted dinucleotides and 2-aminopurine substituted DNA duplexes Phys. Chem. Chem. Phys. 6 154–60
[19] Somsen O J G, Hoek V A and Amerongen V H 2005 Fluorescence quenching of 2-aminopurine in dinucleotides Chem. Phys. Lett. 402 61–5
[20] Wan C, Xia T, Becker H-C and Zewail A H 2005 Ultrafast unequilibrated charge transfer: a new channel in the quenching of fluorescent biological probes Chem. Phys. Lett. 412 158–63
[21] Liang J, Nguyen Q L and Matsika S 2013 Exciplexes and conical intersections lead to fluorescence quenching in [small pi]-stacked dimers of 2-aminopurine with natural purine nucleobases Photochemical {&} Photobiological Sciences 12 1387–400
[22] Liang J and Matsika S 2011 Pathways for fluorescence quenching in 2-Aminopurine π-stacked with pyrimidine nucleobases JACS 133 6799–808
[23] Rachofsky E L, Osman R and Ross J B 2001 Probing structure and dynamics of DNA with 2-aminopurine: effects of local environment on fluorescence Biochemistry 40 946–56
[24] Narayanan M, Kodali G, Xing Y J and Stanley R J 2010 Photoinduced electron transfer occurs between 2-aminopurine and the DNA nucleic acid monophosphates: results from cyclic voltammetry and fluorescence quenching J. Phys. Chem. B 114 10573–80
[25] Voltz K et al 2016 Quantitative sampling of conformational heterogeneity of a DNA hairpin using molecular dynamics simulations and ultrafast fluorescence spectroscopy Nucleic Acids Res. 44 3408–19
[26] Lakowicz J R 2006 Principles of Fluorescence Spectroscopy 3rd ed. (Berlin: Springer)
[27] Smith D A, McKenzie G, Jones A C and Smith T A 2017 Analysis of time-correlated single photon counting data: a comparative evaluation of deterministic and probabilistic approaches Methods. Appl. Fluoresc. 5 1–18
[28] Smith D A, Holroyd L F, van Mourik T and Jones A C 2016 A DFT study of 2-aminopurine-containing dinucleotides: prediction of stacked conformations with B-DNA structure Phys. Chem. Chem. Phys. 18 14691–700
[29] Evans K, Xu D, Kim Y and Nordlund T M 1992 2-Aminopurine optical spectra: solvent, pentose ring, and DNA helix melting dependence Journal of Fluorescence 2 209–16
[30] Jean J M and Krueger B P 2006 Structural fluctuations and excitation transfer between adenine and 2-aminopurine in single-stranded deoxytrinucleotides The Journal of Physical Chemistry B 110 2899–909
[31] Rachofsky E L, Seibert E, Stivers J T, Osman R and Ross J B A 2001 Conformation and dynamics of abasic sites in DNA investigated by time-resolved fluorescence of 2-aminopurine Biochemistry 40 957–67
[32] Gao M et al 2017 Temperature and pressure limits of guanosine monophosphate self-assemblies Sci. Rep. 7 9864
[33] Alev-Behmoaras T, Toulmé J J and Hélène C 1979 Effect of phosphate ions on the fluorescence of tryptophan derivatives. Implications in fluorescence investigation of protein-nucleic acid complexes Biochimie 61 957–60
[34] Pal H, Palit D K, Mukherjee T and Mittal J P 1990 Some aspects of steady state and time-resolved fluorescence of tyrosine and related compounds J. Photochem. Photobiol., A 52 391–409
[35] Vdovenko S I, Kolycheva M T, Gerus I I and Kukhar V P 1993 Influence of phosphate ion on the fluorescence of 3-fluorotyrosine Amino Acids 4 303–6